

# Receptor-Mediated Activation of Heterotrimeric G-Proteins in Living Cells

Chris Janetopoulos,\* Tian Jin,\* Peter Devreotes\*†

Receptor-mediated activation of heterotrimeric GTP-binding proteins (G-proteins) was visualized in living *Dictyostelium discoideum* cells by monitoring fluorescence resonance energy transfer (FRET) between  $\alpha$ - and  $\beta$ - subunits fused to cyan and yellow fluorescent proteins. The G-protein heterotrimer rapidly dissociated and reassociated upon addition and removal of chemoattractant. During continuous stimulation, G-protein activation reached a dose-dependent steady-state level. Even though physiological responses subsided, the activation did not decline. Thus, adaptation occurs at another point in the signaling pathway, and occupied receptors, whether or not they are phosphorylated, catalyze the G-protein cycle. Construction of similar energy-transfer pairs of mammalian G-proteins should enable direct in situ mechanistic studies and applications such as drug screening and identifying ligands of newly found G-protein-coupled receptors.

Chemoattractants, hormones, neurotransmitters, odorants, and other sensory stimuli exert their effects on cells through a vast family of serpentine G-protein-coupled receptors (GPCRs). Excited receptors catalyze the exchange of guanosine triphosphate (GTP) for guanosine diphosphate (GDP) and the dissociation of the G-protein heterotrimer, allowing both the GTP-bound  $\alpha$  subunit and free  $\beta\gamma$  complexes to signal to downstream effectors. The intrinsic guanosine triphosphatase (GTPase) activity of the  $\alpha$ -subunit hydrolyzes the bound GTP and the heterotrimer reassociates, completing the cycle (1, 2). These mechanisms have been derived from studies using isolated membranes and purified proteins and have not yet been directly observed in living cells.

In shallow gradients of chemoattractants, cells such as *D. discoideum* amoebae and leukocytes can activate physiological responses selectively at the cell's leading edge even when the chemoattractant receptors and G-proteins are distributed uniformly on the plasma membrane (3–6). The tightly restricted localization of the physiological responses requires a global adaptation process that also causes the responses to rapidly subside during persistent stimulation. Does global adaptation occur at the level of the G-protein cycle or at a subsequent step? To determine the kinetics and to localize sites of G-protein activation in cells and tissues, we developed a method to directly visualize G-protein dis-

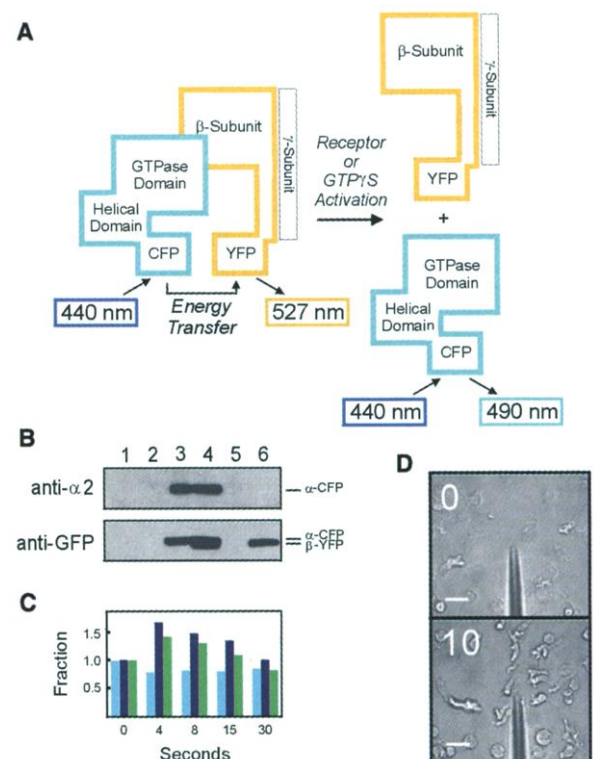
sociation. We reasoned that fluorescence resonance energy transfer (FRET) between probes attached to the  $\alpha$  and  $\beta\gamma$  subunits would allow real-time measurements and imaging of G-protein signaling (7). To test this strategy, we tagged  $\alpha 2$  and  $\beta\gamma$  of *D. discoideum* with cyan and yellow fluorescent

**Fig. 1.** Functional interaction of  $\beta\gamma$ -YFP and  $\alpha 2$ -CFP in living cells. **(A)** CFP was inserted into the helical domain of  $\alpha 2$  in a location optimal for FRET with YFP fused to the  $\text{NH}_2$ -terminus of  $\beta\gamma$  (36). **(B)** Lysates of  $\alpha 2^-$  (lane 1), wild-type (lane 2),  $\alpha 2$ -CFP/ $\alpha 2^-$  (lane 3),  $\alpha 2$ -CFP: $\beta$ -YFP cells (lane 4),  $\beta\gamma^-$  cells (lane 5), and  $\beta\gamma$ -YFP/ $\beta\gamma^-$  cell lines (lane 6) were subjected to immunoblot analyses.  $\alpha 2$  antisera detect an appropriate band in wild-type cells (not shown) and a band at 72 kD in the  $\alpha 2$ -CFP/ $\alpha 2^-$  and  $\alpha 2$ -CFP: $\beta$ -YFP cells. Antisera against GFP (Clontech, Palo Alto, CA) recognize the  $\alpha 2$ -CFP band at 72 kD in the  $\alpha 2$ -CFP/ $\alpha 2^-$  cells, a doublet of the 72-kD band and a 70-kD band of  $\beta\gamma$ -YFP in the  $\alpha 2$ -CFP: $\beta$ -YFP cells, and the 70-kD band in the  $\beta\gamma$ -YFP/ $\beta\gamma^-$  cells. **(C)** In vivo actin polymerization assays of  $\alpha 2^-$  (light blue), wild-type (dark blue), and  $\alpha 2$ -CFP: $\beta$ -YFP (green) cells were carried out as previously described (37). Cells were stimulated with 100 nM cAMP at  $t = 0$  and fixed at times shown. Mean values for an experiment done in duplicate are shown. Two other independent experiments were performed and yielded similar results. **(D)** Cells were differentiated with repeated cAMP stimuli for 6 hours and were then examined for chemotactic response in a micropipette assay. At  $t = 0$ , a micropipette was filled with 1  $\mu\text{M}$  cAMP and placed on the surface of the coverglass. The positions at time 0 and 10 min are shown. Bar, 10  $\mu\text{m}$ .

proteins and used FRET to observe the state of the G-protein heterotrimer in living cells (8).

We assessed the activities of the fusion proteins by phenotypic rescue of  $\alpha 2$  and  $\beta\gamma$  null cell lines. Fusion of enhanced yellow fluorescent protein (YFP) to the  $\text{NH}_2$ -terminus of  $\beta\gamma$  did not impair the capacity of  $\beta\gamma$  to rescue the chemotactic defects of  $\beta\gamma$  null mutants ( $\beta\gamma^-$  cells) (6, 9). Guided by the crystal structures of several mammalian heterotrimers (10, 11), we inserted the enhanced cyan fluorescent protein (CFP) into the first loop (between  $\alpha A$  and  $\alpha B$ ) of the helical domain of  $\alpha 2$ . Mutants that do not express  $\alpha 2$  ( $\alpha 2^-$  cells) are completely deficient in chemoattractant-induced responses and therefore are unable to aggregate and differentiate (12). Stable expression of  $\alpha 2$ -CFP rescued the chemotactic and developmental defects of the  $\alpha 2^-$  cells (13). Chemoattractants triggered in vivo actin polymerization, and chemoattractant-filled micropipettes induced chemotactic responses. Similarly, co-transformation with  $\alpha 2$ -CFP and  $\beta\gamma$ -YFP rescued the  $\alpha 2^-$  cells (Fig. 1) (14).

Studies of cell lines expressing fluorescent subunits showed direct, specific transfer of resonance energy from  $\alpha 2$ -CFP to  $\beta\gamma$ -YFP when the two proteins were co-expressed (Fig. 2A). We excited living, differ-



Department of Biological Chemistry, Johns Hopkins Medical Institutions, Baltimore, MD 21205, USA.

\*Present address: Department of Cell Biology and Anatomy, Johns Hopkins Medical Institutions, Baltimore, MD 21205, USA.

†To whom correspondence should be addressed.

entiated cells at 440 nm and recorded the emission spectrum between 460 and 600 nm. The co-transformed cells showed an extra emission peak near 527 nm, corresponding to the FRET fluorescence (15). Cell lines expressing  $G\alpha 2$ -CFP alone or mixtures of cells containing either  $G\alpha 2$ -CFP or  $G\beta$ -YFP alone did not display this additional peak. Co-transformation of  $G\alpha 2$ -CFP and  $G\beta$ -YFP into  $g\beta^-$  cells gave similar results; here, we focused on the co-transformed  $g\alpha 2^-$  cells (designated  $\alpha 2$ -CFP: $\beta$ -YFP cells). The FRET fluorescence was observed in both membrane and supernatant fractions prepared from  $\alpha 2$ -CFP: $\beta$ -YFP cells, suggesting heterotrimers exist in the cytoplasm as well as on the plasma membrane. The FRET fluorescence disappeared after treatment of membranes with  $Mg^{2+}$  plus GTP- $\gamma$ -S, but not with GTP- $\gamma$ -S alone (16).

Addition of the chemoattractant cyclic adenosine 3',5' monophosphate (cAMP) to  $\alpha 2$ -CFP: $\beta$ -YFP cells triggered a rapid, substantial loss of FRET fluorescence reflecting receptor-mediated activation and dissociation of the G-protein heterotrimer (Fig. 2B). There was a decrease in the YFP emission signal near 527 nm and a parallel increase in the CFP emission signals near 475 and 501 nm. The 490:527 ratio increased by 32%; the

FRET fluorescence decreased by about 70% (17). Only  $\alpha 2$ -CFP: $\beta$ -YFP cells showed a change in fluorescence intensity when stimulated (18). The large decrease suggests that the heterotrimer may dissociate rather than merely change conformation. We measured the kinetics of loss and restoration of the FRET fluorescence upon addition and removal of the stimulus (Fig. 2C). The response was maximal within 10 s of stimulation, the earliest time point taken. In other experiments, the response reached 90% of the maximum within a few seconds (16). As the cAMP was removed by the endogenous phosphodiesterase, the FRET fluorescence returned to its maximal level within 2 min. Activation is at least as fast as the most rapid receptor-mediated physiological responses such as actin polymerization and Pleckstrin homology (PH)-domain translocation.

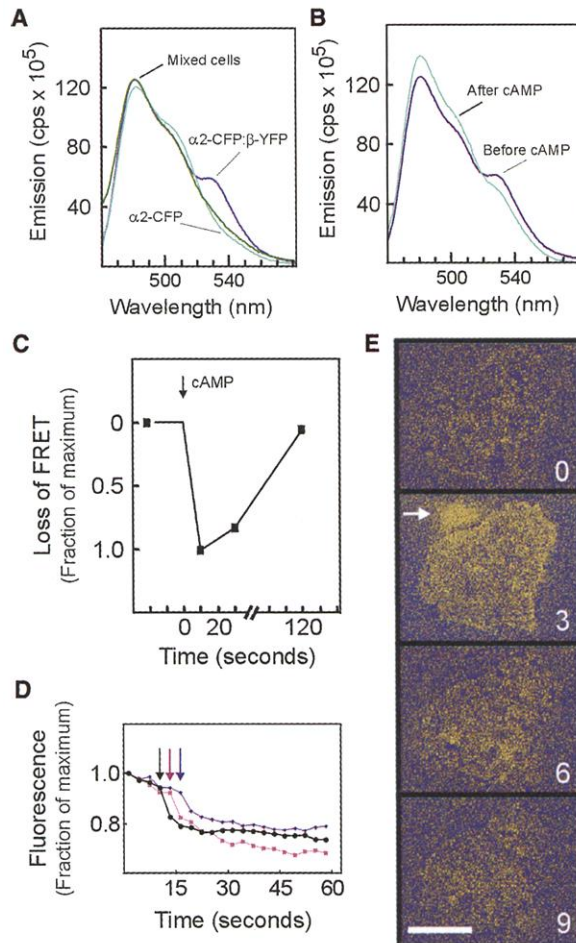
We attempted to directly visualize the change in the FRET fluorescence by conventional fluorescence microscopy. When  $\alpha 2$ -CFP: $\beta$ -YFP cells were excited with blue light (420 to 460 nm) and observed in the yellow range (525 to 540 nm), there was a fluorescent signal on the membrane as well as within the cell perimeter (Fig. 2, D and E). These fluorescent signals were lower in cells expressing  $\alpha 2$ -CFP or  $\beta$ -YFP alone, even

though these cells were highly fluorescent when examined with the appropriate cyan or yellow filter sets. When a saturating dose of cAMP was added to the  $\alpha 2$ -CFP: $\beta$ -YFP cells, the membrane signal decreased by about 15% within 6 s and did not reappear during the 1-min period of observation. The signal within the perimeter of the cell also displayed a slight decrease. We visualized the response by subtracting consecutive frames from one another (Fig. 2E). These microscopy results extend and confirm the fluorometric observations.

Treatment with increasing concentrations of cAMP and two of its analogs, 2' deoxyadenosine-3',5' monophosphate (2'-dcAMP) and 8-bromoadenosine-3',5' monophosphate (8-Br-cAMP) decreased the FRET fluorescence in a dose-dependent manner (Fig. 3). To quantitate the response for each analog, we subtracted the spectrum for the highest concentration from that of each of the lower concentrations. The negative values from 475 to 520 nm reflect the gain in cyan fluorescence, and the positive values from 520 to 550 nm reflect the loss in yellow fluorescence (Fig. 3A; see also Fig. 2B). Processing of this data yielded  $EC_{50}$ s for cAMP, 2'-dcAMP, and 8-Br-cAMP of about 10 nM, 20 nM, and 2  $\mu$ M, respectively, which were shifted to the left of their reported binding affinities (average  $K_D$ s  $\approx$  180 nM, 1  $\mu$ M, and 32  $\mu$ M, respectively) (19). This suggests that the steady-state level of G-protein activation saturates before all receptors are fully occupied and favors the possibility that the receptors act catalytically (20). Addition of 1 mM 5'-AMP, which does not bind to the cAMP receptor (cAR1), had no effect on the FRET fluorescence. These data validate the hypothesis, based on previous genetic studies (12), that the heterotrimeric G-protein formed from  $G\alpha 2$  [1 of 11 known  $\alpha$ -subunits in *D. discoideum* (21, 22)] and the unique  $\beta\gamma$ -complex are directly linked to the cAMP chemoattractant receptors.

Prolonged stimulation of *D. discoideum* cells with cAMP induces adaptation of a number of physiological responses, such as actin polymerization and PH-domain recruitment to the plasma membrane (23). Yet previous studies have suggested that receptors remain coupled to G-proteins in adapted cells (24). To examine adaptation of the G-protein heterotrimer, we persistently stimulated  $\alpha 2$ -CFP: $\beta$ -YFP cells with 100 nM cAMP for 18 min. Half the cells were left to recover in the absence of cAMP and half were exposed to 10  $\mu$ M cAMP for an additional 10 min. During the first 18 min of treatment, the FRET fluorescence in living cells decreased and remained near 20% of the initial value (Fig. 4A) (25). Cells that were no longer exposed to cAMP after 18 min showed a gradual increase in FRET fluorescence, reflecting the

**Fig. 2.** Fluorescence spectra of cell lines. (A)  $G\alpha 2$ -CFP/ $g\alpha 2^-$  cells (light blue),  $\alpha 2$ -CFP: $\beta$ -YFP cells (dark blue), and mixture of equal number of  $G\alpha 2$ -CFP/ $g\alpha 2^-$  and  $G\beta$ -YFP/ $g\beta^-$  cells (green) were excited in a Spex Fluoromax-2 fluorimeter at 440 nm and emission spectra were collected and processed (15). (B) Emission spectra from  $\alpha 2$ -CFP: $\beta$ -YFP cells before (dark blue) and after (light blue) treatment with 100  $\mu$ M cAMP. (C) Kinetics of transient loss of FRET fluorescence after addition of 100  $\mu$ M cAMP to  $\alpha 2$ -CFP: $\beta$ -YFP cells (38). (D) Cells were observed with excitation and emission bandpass filters of 420 nm to 450 nm (Chroma Exciter 436/20) and 520 nm to 550 nm (Chroma Emitter 535/30), respectively. Mean intensities were calculated in IPLab Spectrum by manually circumscribing the membrane of multiple cells. The three curves represent individual cells from three different video sequences. Arrows indicate the frame at which the stimulus was added. (E) Difference images of consecutive frames captured at 3 s intervals were calculated in IPLab Spectrum. Stimulus was added between frames labeled 0 and 3 s; small cell indicated by the arrow was dislodged by the disturbance. Bar, 10  $\mu$ m.



REPORTS

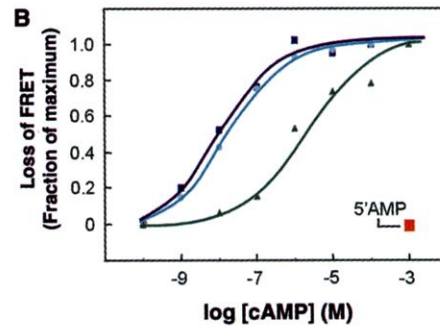
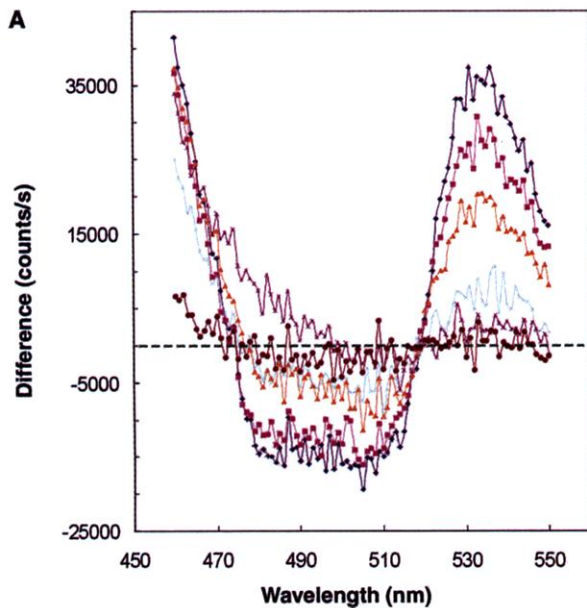


**Fig. 3.** Dose-response curves for cAMP, 2'-dcAMP, 8-Br cAMP and 5' AMP. (A) Difference fluorescence spectrum of  $\alpha 2$ -CFP:  $\beta$ -YFP cells treated with increasing concentrations of cAMP. Cells were treated with caffeine and stimulated with 0 (dark blue), 1 nM (magenta), 10 nM (orange), 100 nM (light green), 1  $\mu$ M (violet), 10  $\mu$ M (brown), and 100  $\mu$ M cAMP (dashed line) in the presence of 10 mM dithiothreitol, and analyzed in the flu-

orimeter 15 s after mixing. (B) Dose-response curves for cAMP (dark blue), 2'-dcAMP (light blue), and 8-Br cAMP (green), and 5' AMP (orange). Data from two independent experiments were averaged for each curve. Data was processed as described (39).

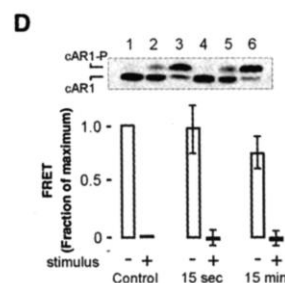
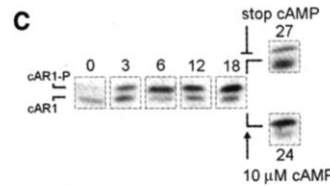
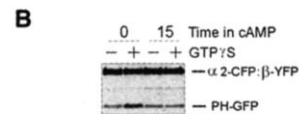
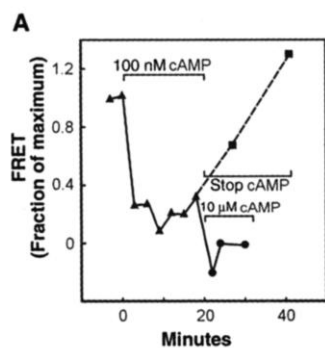
gradual degradation of cAMP by endogenous phosphodiesterase. Cells treated with 10  $\mu$ M cAMP showed a further decrease in FRET fluorescence. In lysates from naïve  $\alpha 2$ -CFP:  $\beta$ -YFP cells, GTP- $\gamma$ -S stimulated the binding of PH-domains to membranes (3, 26). This response was lost in cells pretreated with cAMP (Fig. 4B), indicating that these cells adapt normally. Because persistent stimulation does not return the G-proteins to the heterotrimeric or "off" position, adaptation of the physiological responses must occur at another point in the signaling pathway.

The persistent activation of the G-protein cycle is surprising because agonist-induced phosphorylation of the receptors reaches a plateau within a few minutes (27). Immunoblots of selected time points showed the expected steady-state level of receptor phosphorylation (Fig. 4C). Next, sets of cells were stimulated with cAMP for 0, 15 s, or 15 min and then washed at 0°, a condition known to prevent receptor dephosphorylation (Fig. 4D, inset). After washing, the FRET fluorescence of the three sets of cells was nearly identical, indicating that the G-protein heterotrimer re-

associated even though receptors remained phosphorylated. Subsequent stimulus addition caused a parallel loss of FRET fluorescence in each set of cells (Fig. 4D). Agonist-induced phosphorylation of other GPCRs facilitates a series of downstream events such as arrestin binding that uncouple excited receptors from G-proteins (28–31). Phosphorylation of cAR1 decreases its affinity for cAMP (32); however, the low affinity receptors continue to trigger the G-protein cycle.

The evidence presented here is consistent with the model of the steady-state G-protein cycle derived from in vitro measurements, although a mechanism of adaptation is absent (1). The rapid kinetics, reversibility, and dose-dependence suggest that occupied receptors repeatedly elicit G-protein activation. It is expected that regulators of G-protein signaling (RGS proteins) will influence the steady-state ratio of active and inactive G-proteins (33, 34) and not shape the time courses of the physiological responses because adaptation does not directly involve the G-protein cycle. The persistent kinetics of G-protein activation suggests that its spatial pattern likely reflects the shallow external gradient of receptor occupancy rather than the tightly restricted localization of the physiological responses. Thus, restriction of the response to the cell's leading edge may involve pathways beyond or independent from the G-protein cycle.

**Fig. 4.** Continuous activation of the G-protein cycle. (A)  $\alpha 2$ -CFP:  $\beta$ -YFP cells were treated with 3 mM caffeine and were maintained at 100 nM cAMP by adding fresh cAMP every minute for 18 min and then divided into two sets. One set received no further cAMP, whereas the second was increased to 10  $\mu$ M cAMP. Spectra were processed as described (39). (B) Cells were treated with cAMP for 0 or 15 min, lysed, and then incubated in the presence or absence



of GTP- $\gamma$ -S with a supernatant from cells expressing PH<sub>CRAC</sub>-GFP (3). After 2 min, membranes were collected and binding of the PH<sub>CRAC</sub>-GFP was assessed by immunoblot analysis using antibodies to GFP. (C) Immunoblot analysis shows separation of the cAR1 doublet into its lower (phosphorylated) and higher (nonphosphorylated) mobility forms (32). (D) Identical sets of cells received buffer (control), one addition of 100  $\mu$ M cAMP for 15 s (15 sec), or 15 additions, once per minute (15 min). All sets were then washed at 0°. Bars show the fraction ( $\pm$ SD) of FRET fluorescence before (-) and after (+) addition of a second cAMP stimulus (10  $\mu$ M). Immunoblot analyses of cAR1 in samples taken after washing and before restimulation show control (lanes 1 and 4), 15 s treated (lanes 2 and 5), and 15 min treated (lanes 3 and 6). The average fraction of unphosphorylated receptor remaining after 0, 15 s, and 15 min were 100, 89, and 9%, respectively. Duplicate experiments performed on different days were averaged.

References and Notes

1. A. G. Gilman, *Annu. Rev. Biochem.* **56**, 615 (1987).
2. H. E. Hamm, *J. Biol. Chem.* **273**, 669 (1998).
3. C. A. Parent, B. J. Blacklock, W. M. Froehlich, D. B. Murphy, P. N. Devreotes, *Cell* **95**, 81 (1998).
4. Z. Xiao, N. Zhang, D. B. Murphy, P. N. Devreotes, *J. Cell Biol.* **139**, 365 (1997).

5. G. Servant *et al.*, *Science* **287**, 1037 (2000).
6. T. Jin, N. Zhang, Y. Long, C. A. Parent, P. N. Devreotes, *Science* **287**, 1034 (2000).
7. R. R. Neubig, M. P. Connolly, A. E. Remmers, *FEBS Lett.* **355**, 251 (1994).
8. R. Heim, R. Y. Tsien, *Curr. Biol.* **6**, 178 (1996).
9. The gene encoding the full-length YFP was fused to the NH<sub>2</sub>-terminus of the G $\beta$  gene. A Bgl II restriction site was added at the junction that consisted of two additional amino acids, arginine and serine. This  $\beta$ -YFP fusion protein was cloned into the CV5 vector. CV5 was derived from p88 by addition of an actin 15 expression cassette from pMC34 (3).
10. D. G. Lambright *et al.*, *Nature* **379**, 311 (1996).
11. M. A. Wall *et al.*, *Cell* **83**, 1047 (1995).
12. A. Kumagai *et al.*, *Cell* **57**, 265 (1989).
13. The gene encoding the full-length CFP was inserted into a Spe I site after residue 90, in the loop between the  $\alpha$ A and the  $\alpha$ B helices, of the G $\alpha$ 2 cDNA. The Spe I site also added a threonine and serine residue at the NH<sub>2</sub>- and COOH-terminal boundaries of the insertion, respectively. This fusion was cloned into the CV5 vector. The  $\alpha$ 2<sup>-</sup> cells were transformed, and individual G418 resistant clones were selected. Rescued cells formed fruiting bodies and viable spores.
14. Equal amounts of plasmids carrying the G $\alpha$ 2-CFP and G $\beta$ -YFP fusions were mixed and transformed into  $\alpha$ 2<sup>-</sup> cells. Individual G418 resistant clones were selected. Greater than 90% of transformed cells expressed both proteins.
15. The magnitude of the FRET fluorescence compared with that of G $\beta$ -YFP directly excited at 490 nm and not relayed through G $\alpha$ 2-CFP varied from 7% (Fig. 2) to 12%. Emission spectra were collected between 460 and 600 nm (excitation at 440 nm) of the following lines:  $\alpha$ 2-CFP: $\beta$ -YFP, a mixture of G $\alpha$ 2-CFP/ $\alpha$ 2<sup>-</sup> and G $\beta$ -YFP/ $\alpha$ 2<sup>-</sup>, and wild-type (AX3). Spectra were normalized to the fluorescence at 600 nm of the  $\alpha$ 2-CFP: $\beta$ -YFP cells, and the wild-type spectrum was subtracted from the others. The corrected spectra were normalized to the fluorescence at 490 nm of the  $\alpha$ 2-CFP: $\beta$ -YFP cells (see Fig. 2A). The amount of FRET fluorescence was determined by subtracting from the spectrum of the  $\alpha$ 2-CFP: $\beta$ -YFP cells either the spectrum of the mixed cells or that of the G $\alpha$ 2-CFP/ $\alpha$ 2<sup>-</sup> cells. In the latter case, a further correction was made for the fluorescence emitted from G $\beta$ -YFP/ $\alpha$ 2<sup>-</sup> directly excited at 440 nm.
16. C. Janetopoulos, P. N. Devreotes, unpublished data.
17. The residual signal may be due to cytoplasmic heterotrimer or a portion of membrane associated heterotrimer that remains during persistent stimulation.
18. The emission spectra of G $\alpha$ 2-CFP cells (excited at 440 nm), G $\beta$ -YFP cells (excited at 440 or 490 nm), or mixtures of G $\alpha$ 2-CFP cells and G $\beta$ -YFP cells (excited at 440 nm) did not change after stimulation.
19. R. L. Johnson *et al.*, *J. Biol. Chem.* **267**, 4600 (1992).
20. The EC<sub>50</sub>'s of cAMP-induced actin polymerization, adenyl cyclase activation, and calcium influx are 1 nM, 10 nM, and 200 nM, respectively. This suggests that there is a further amplification in the actin response and none in the adenyl cyclase response. Interestingly, the calcium response requires more occupied receptors than does G-protein activation. This is consistent with the observation that the calcium response is partially independent of G-proteins.
21. L. J. Wu, P. N. Devreotes, *Biochem. Biophys. Res. Commun.* **179**, 1141 (1991).
22. S. van Es, P. N. Devreotes, *Cell Mol. Life Sci.* **55**, 1341 (1999).
23. C. A. Parent, P. N. Devreotes, *Annu. Rev. Biochem.* **65**, 411 (1996).
24. E. Snaar-Jagalska, S. van Es, F. Kesbeke, P. J. Van Haastert, *Eur. J. Biochem.* **195**, 715 (1991).
25. In another experiment, we added a single dose of 100  $\mu$ M cAMP plus dithiothreitol to inhibit phosphodiesterase. Activation did not subside during 6 min of observation.
26. P. J. Lilly, P. N. Devreotes, *J. Cell Biol.* **129**, 1659 (1995).
27. R. A. Vaughan, P. N. Devreotes, *J. Biol. Chem.* **263**, 14538 (1988).
28. A. Mendez, N. V. Krasnoperova, J. Lem, J. Chen, *Methods Enzymol.* **316**, 167 (2000).
29. J. Chen, C. L. Makino, N. S. Peachey, D. A. Baylor, M. I. Simon, *Science* **267**, 374 (1995).
30. J. Vinós, K. Jalink, R. W. Hardy, S. G. Britt, C. S. Zuker, *Science* **277**, 687 (1997).
31. R. R. Gainetdinov *et al.*, *Neuron* **24**, 1029 (1999).
32. M. Caterina, P. N. Devreotes, J. Borleis, D. Herold, *J. Biol. Chem.* **270**, 8667 (1995).
33. L. De Vries, B. Zheng, T. Fischer, E. Elenko, M. G. Farquhar, *Annu. Rev. Pharmacol. Toxicol.* **40**, 235 (2000).
34. D. M. Berman, A. G. Gilman, *J. Biol. Chem.* **273**, 1269 (1998).
35. A. B. Cubitt, R. Heim, L. A. Woollenweber, *Methods Cell Biol.* **58**, 19 (1999).
36. Enhanced CFP is a class 5 (F64L, S65T, Y66W, N146I, M153T, V163A) and the enhanced YFP is a class 4 (S65G, V68L, S72A, T203Y) GFP variant (35).
37. S. H. Zigmond, M. Joyce, J. Borleis, G. M. Bokoch, P. N. Devreotes, *J. Cell Biol.* **138**, 363 (1997).
38. Cells were scanned between 515 and 540 nm, normalized to the fluorescence at 527 nm of a 460- to 600-nm emission spectrum of  $\alpha$ 2-CFP: $\beta$ -YFP cells (no cAMP). Spectra were corrected by subtraction of a normalized wild-type spectrum.
39. Spectra were first normalized to the integral from 475 to 550 nm. The spectrum at the highest dose was then subtracted from each of the other spectra. The areas under the differences curves were integrated from 475 to 520 nm and from 520 to 550 nm, and the absolute values were summed.
40. The authors wish to thank S. van Es, C. A. Parent, and L. Tang for advice and assistance in designing constructs and D. Murphy for help with the microscopy. Supported by NIH grants GM28007 and GM34933 to P.N.D. and an ACS Fellowship to C.J.

15 September 2000; accepted 12 February 2001

## Length of the Flagellar Hook and the Capacity of the Type III Export Apparatus

Shigeru Makishima,<sup>1</sup> Kaoru Komoriya,<sup>2</sup> Shigeru Yamaguchi,<sup>3</sup> Shin-ichi Aizawa<sup>1\*</sup>

Length determination in biology generally uses molecular rulers. The hook, a part of the flagellum of motile bacteria, has an invariant length. Here, we examined hook length and found that it was determined not by molecular rulers but probably by the amount of subunit protein secreted by the flagellar export apparatus. The export apparatus shares common features with the type III virulence-factor secretion machinery and thus may be used more widely in length determination of structures other than flagella.

The bacterial flagellum, a rotary device for motility, is a supramolecular structure consisting of more than 20 different proteins that build up into three distinctive substructures: the filament, hook, and basal structure (1, 2). In *Salmonella enterica* serovar Typhimurium, the hook has an average length of 55 nm with a standard deviation of 6 nm (3), whereas the filament length varies over a wide range. In order to elucidate the mechanism regulating the invariant length of the hook, we used mutants that give rise to hooks of indefinite length, called "polyhooks." The mutation sites in these strains are not in the hook protein gene (*flgE*) but are in the *fliK* gene, suggesting that FliK acts as a length controller or a molecular ruler of the hook (4–7).

If FliK were a simple molecular ruler, truncated FliK's should produce shorter, not longer, hooks. However, all *fliK* mutants so far studied give rise to long polyhooks (8). In order to identify what controls the hook length, it is necessary to find mutants that produce short

hooks. After an extensive survey, we found such strains with mutations in the *fliG*, *fliM*, and *fliN* genes.

Mutation in these three genes gives rise to different phenotypes, depending on the degree of their defects: Fla<sup>-</sup> (filament-less) mutants derive from major defects, and Mot<sup>-</sup> (motility-less) or Che<sup>-</sup> (chemotaxis-less) mutants are from minor defects (9, 10). These three genes are commonly called the switch genes, putting an emphasis on the behavioral phenotype Che<sup>-</sup>, in which the switch mechanism of the motor rotation is perturbed.

In the early stage of the survey by electron microscopy, we found short hooks in the intact flagella isolated from *fliG* mutants with Che<sup>-</sup> phenotypes (Fig. 1A). The hook portion of the flagella looked less curved than that of the wild type, implying the shortness of the hook. In order to reveal the hook length more explicitly, hook-basal bodies (HBBs) were isolated (Fig. 1B), and the hook lengths were measured to produce diagrams of length distribution. The hook length of SJW2325 (*fliG*/Che<sup>-</sup>) was 26.8  $\pm$  8.0 nm, about half the length of the wild type (Fig. 2A).

Next, we isolated HBBs from both Che<sup>-</sup> and Mot<sup>-</sup> mutants of all the switch genes in our collection (three *fliG*/Che<sup>-</sup>, seven *fliM*/Che<sup>-</sup>, one *fliN*/Che<sup>-</sup>, two *fliG*/Mot<sup>-</sup>, five *fliM*/Mot<sup>-</sup>,

<sup>1</sup>Department of Biosciences, Teikyo University, 1-1 Toyosatodai, Utsunomiya 320-8551, Japan. <sup>2</sup>Department of Applied Biochemistry, Utsunomiya University, Utsunomiya 321-8505, Japan. <sup>3</sup>Izumi Campus, Meiji University, 1-9-1 Eifuku, Suginami, Tokyo 168-0064, Japan.

\*To whom correspondence should be addressed. E-mail: aizawa@nasu.bio.teikyo-u.ac.jp